Zeros of Loschmidt echo in the presence of Anderson localization

Honghao Yin,[1] Shu Chen,[2] Xianlong Gao,[1] and Pei Wang[1,*]

[1]*Department of Physics, Zhejiang Normal University, Jinhua 321004, People's Republic of China*

[2]*Beijing National Laboratory for Condensed Matter Physics, Institute of Physics, Chinese Academy of Sciences, Beijing 100190, China*

(Received 30 December 2017; revised manuscript received 5 February 2018; published 28 March 2018)

We study the Loschmidt echo and the dynamical free energy of the Anderson model after a quench of the disorder strength. If the initial state is extended and the eigenstates of the postquench Hamiltonian are strongly localized, we argue that the Loschmidt echo exhibits zeros periodically with the period $2\pi/D$, where D is the width of spectra. At these zeros, the dynamical free energy diverges in a logarithmic way. We present numerical evidence of our argument in one- and three-dimensional Anderson models. Our findings connect the dynamical quantum phase transitions to the localization-delocalization phase transitions.

DOI: 10.1103/PhysRevA.97.033624

I. INTRODUCTION

Since Anderson's seminal paper in 1958 [1], Anderson localization has been extensively studied. In recent years, great progress was made in simulating the nonequilibrium dynamics of closed quantum systems by using ultracold atoms [2]. A question then arises as to what the influence is of Anderson localization on the nonequilibrium dynamics. An especially interesting protocol of driving a system out of equilibrium is by a quantum quench, i.e., by suddenly changing the Hamiltonian of the system. For a homogeneous integrable system such as a noninteracting Fermi gas, the local observable relaxes to a steady value after a quench [3,4]. And this steady value can be predicted by the generalized Gibbs ensemble (GGE) [3]. But if the postquench Hamiltonian has localized eigenstates, the observable exhibits an everlasting oscillation with its average deviating significantly from the prediction of GGE [5–9]. This everlasting oscillation comes from the pure-point spectrum associated with the localized eigenstates [7].

An important quantity characterizing the nonequilibrium dynamics is the Loschmidt echo

$$\mathcal{L}(t) = \langle\Psi(0)|e^{-i\hat{H}t}|\Psi(0)\rangle, \tag{1}$$

where $|\Psi(0)\rangle$ denotes the prequench quantum state and $\hat{H}$ is the postquench Hamiltonian. $\mathcal{L}(t)$ might become zero at some critical times t^*, at which the dynamical free energy in thermodynamic limit is nonanalytic. The dynamical free energy is usually defined as

$$f(t) = -\lim_{N\to\infty}\frac{1}{N}\ln|\mathcal{L}(t)|^2, \tag{2}$$

where N denotes the number of particles. The nonanalyticity of $f(t)$ at $t = t^*$ is dubbed a dynamical quantum phase transition (DQPT) [10].

Ever since the original paper of Heyl *et al.* [10], the DQPTs have been theoretically addressed in various models [11–19] with the experimental observations also realized recently [20,21]. It was argued that the Loschmidt echo exhibits zeros if the prequench and postquench Hamiltonians have topologically different ground states [18], or if the prequench state breaks some symmetry which is recovered after the quench [19]. The relation between the DQPTs and the topological phase transitions (or the symmetry-breaking phase transitions) is then established.

While most theoretical works on DQPTs focus on the quantum systems with phase transitions caused by broken symmetries or accompanied by the close of energy gap, DQPTs driven by disorders are rarely studied except of a recent work on the one-dimensional Aubry–André model with quasiperiodic potentials [22]. In this paper we make a further step towards connecting the DQPTs to the localization-delocalization transitions. This is done by proving that zeros of Loschmidt echo and nonanalyticity of the dynamical free energy occur if an extended initial state is quenched into a strongly localized regime. Besides a proof based on the properties of the wave functions and the spectrum in a localized phase, we also provide numerical evidence in one- and three-dimensional Anderson models. Different from the quasiperiodic system with deterministic quasirandom potentials, we will discuss the more general disordered systems with random potentials of white-noise type and focus our study on the quench dynamics from an initial extended state to the strongly disordered regime. We find that the critical times in the case of white-noise potentials are $t_n^* = \frac{2\pi n}{D}$ with n an integer and D the spectrum width of $\hat{H}$, which are different from the critical times in the case of quasiperiodic potentials—the zeros of the Bessel function [22]. Our results will serve as a benchmark for understanding the characteristics of the Loschmidt echo and the dynamical free energy after a more general quench with the initial and the postquench Hamiltonians at arbitrary disorder strength.

The contents of the paper are arranged as follows: In Sec. II, we present a general argument about the zeros of the Loschmidt echo and the nonanalyticity of the dynamical free energy. The numerical evidence is given in Sec. III. In Sec. IV, we discuss the feature of the wave function before or after each zero of the Loschmidt echo. Section V is a short summary.

*wangpei@zjnu.cn

II. DYNAMICAL QUANTUM PHASE TRANSITION IN STRONG-DISORDER LIMIT

The Hamiltonian of the Anderson model is in general expressed as

$$\hat{H} = -g \sum_{\langle i,j \rangle} (\hat{a}_i^\dagger \hat{a}_j + \text{H.c.}) + \sum_i u_i \hat{a}_i^\dagger \hat{a}_i, \tag{3}$$

where $\langle i,j \rangle$ denotes a pair of neighbor sites and u_i is the on-site potential which is an independent random number distributed uniformly in the interval $[-W/2, W/2]$ with W denoting the disorder strength. g is set to the unit of energy throughout the paper. We focus on bosons in this paper. $\hat{a}_i^\dagger$ and $\hat{a}_i$ denote the bosonic creation and annihilation operators, respectively.

Let us suppose that the system is initially prepared in an extended state; e.g., in the ground state of the Hamiltonian (3) at $W = 0$. In the initial state, all the bosons occupy the lowest energy level, the single-particle wave function of which is denoted as $|\phi(0)\rangle$. The system is then driven out of equilibrium by suddenly changing the Hamiltonian to $\hat{H}$ at finite W. Since we do not consider the interaction between bosons, the many-body wave function keeps a product state during the time evolution. Furthermore, all the bosons have the same wave function at arbitrary time, which is denoted as $|\phi(t)\rangle$. We use $|\alpha_n\rangle$ to denote the single-particle eigenstate of the postquench Hamiltonian with the corresponding eigenenergy ϵ_n, where $n = 1,2,\ldots,L$ and L is the total number of sites. We then obtain

$$|\phi(t)\rangle = \sum_{n=1}^{L} \langle \alpha_n | \phi(0) \rangle \, e^{-i\epsilon_n t} \, |\alpha_n\rangle \, . \tag{4}$$

If the system contains N bosons, the Loschmidt echo of the many-body wave function becomes

$$\begin{aligned} \mathcal{L}(t) &= \langle \phi(0) | \phi(t) \rangle^N \\ &= \left(\sum_{n=1}^{L} |\langle \phi(0) | \alpha_n \rangle|^2 e^{-i\epsilon_n t} \right)^N . \end{aligned} \tag{5}$$

Now we discuss the case in which the system is quenched into the strongly disordered regime. In this regime, all the single-particle eigenstates $|\alpha_n\rangle$ are strongly localized like a δ function. Recall that the initial single-particle state $|\phi(0)\rangle$ is extended over the whole system like a plane wave. Therefore, the overlap $\langle \phi(0) | \alpha_n \rangle$ is approximately $1/\sqrt{L}$. With this in mind, we find that $|\langle \phi(0) | \alpha_n \rangle|^2$ is $1/L$ which is independent of n. And the Loschmidt echo becomes $\mathcal{L}(t) = l(t)^N$, where the single-particle Loschmidt echo is

$$l(t) = \frac{1}{L} \sum_{n=1}^{L} e^{-i\epsilon_n t}. \tag{6}$$

The sum of $e^{-i\epsilon_n t}$ is determined by the single-particle levels ϵ_n, which depend on the configuration of disorder and are in fact random numbers. Let us study the joint probability density $P(\epsilon_1, \epsilon_2, \ldots, \epsilon_L)$ of these random levels. In the Hamiltonian (3), the disordered potential u_i is a random number uniformly distributed in the range from $-W/2$ to $W/2$. In the localized phase, the probability density of the nearest-neighbor level spacing is the Poisson distribution ($\sim e^{-s}$ with s denoting the spacing between two neighbor levels) which results from $\epsilon_1, \ldots, \epsilon_L$ being independent and uniformly distributed random numbers [23–25]. Therefore, in the localized phase we have

$$P(\epsilon_1, \epsilon_2, \ldots, \epsilon_L) = 1/D^L, \tag{7}$$

where D is the width of the single-particle spectra. In the strong-disorder limit (large-W limit), the disordered potentials govern the Hamiltonian (3), and $\epsilon_1, \ldots, \epsilon_L$ are then no more than the disordered potentials which are of course independent and uniformly distributed random numbers according to the definition. In this limit the width of spectra D is equal to W.

Equipped with the knowledge of $P(\epsilon_1, \epsilon_2, \ldots, \epsilon_L)$, we can now calculate the Loschmidt echo, which after averaged over the level distribution becomes

$$\begin{aligned} l(t) &= \int_{-D/2}^{D/2} d\epsilon_1 \cdots d\epsilon_L \, P(\epsilon_1, \epsilon_2, \ldots, \epsilon_L) \frac{1}{L} \sum_{n=1}^{L} e^{-i\epsilon_n t} \\ &= \frac{e^{-itD/2}(e^{itD} - 1)}{iDt}. \end{aligned} \tag{8}$$

It is clear that both the single-particle and many-body Loschmidt echo vanish periodically at the critical times $t_n^* = 2\pi n/D$ with $n = 1,2,\ldots$ a positive integer. The vanishing of the Loschmidt echo causes the nonanalyticity of the dynamical free energy which, according to Eq. (2), evaluates to

$$f(t) = -\ln \frac{\sin^2(Dt/2)}{(Dt/2)^2}. \tag{9}$$

The dynamical free energy is divergent at the critical times t_n^*. Both the Loschmidt echo and the dynamical free energy signal periodically occurred DQPTs at $t_n^* = 2\pi n/D$. And the dynamical free energy is not continuous at these DQPTs.

III. DYNAMICAL QUANTUM PHASE TRANSITION IN ONE- AND THREE-DIMENSIONAL ANDERSON MODELS

We numerically study the Loschmidt echo and the dynamical free energy for the one- and three-dimensional Anderson Hamiltonians. In our calculation we choose the periodic boundary condition. At $W = 0$, the single-particle eigenstates of the Anderson model are plane waves. In one dimension, the eigenstates are all localized in the presence of infinitesimal W. While in three dimensions, the eigenstates are localized only if the disorder strength W is beyond a critical value W_c. The initial state is set to the ground state of $\hat{H}$ at $W = 0$. A finite W is switched on at $t = 0$ and the Loschmidt echo and the dynamical free energy are then calculated. In the calculation, we perform an average over different disorder configurations by sampling the disorder potentials for many times until the results converge.

Let us first see the single-particle Loschmidt echo $l(t) = \langle \phi(0) | \phi(t) \rangle$. The single-particle eigenenergy at $W = 0$ is $\epsilon = -2g \cos k$ in one dimension or $\epsilon = -2g(\cos k_x + \cos k_y + \cos k_z)$ in three dimensions where k or (k_x, k_y, k_z) denote the wave vectors; thereafter, the ground state $|\phi(0)\rangle$ is a plane wave of zero wave vector. The amplitude of $|\phi(0)\rangle$ at arbitrary site is $1/\sqrt{L}$. Figures 1(a) and 1(b) display the absolute value $|l(t)|$ for the one-dimensional Anderson model at different W and L. The numerical results fit well with Eq. (8) if the disorder

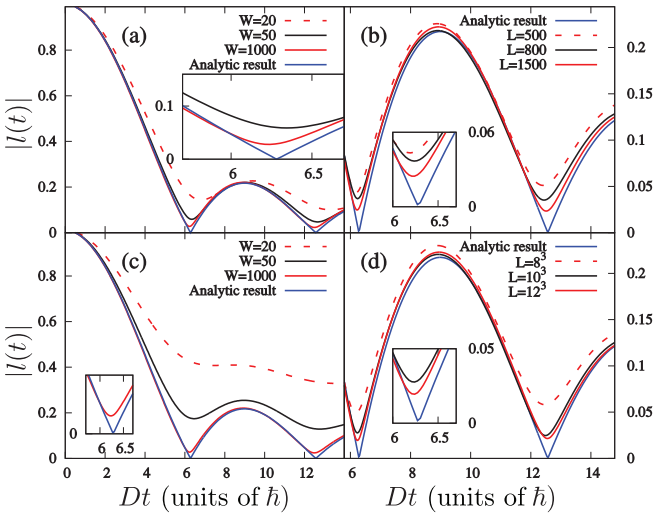

FIG. 1. The absolute value of the Loschmidt echo as a function of time. Panels (a) and (b) are for the one-dimensional Anderson model at different W with fixed $L = 1000$ and at different L with fixed $W = 1000$, respectively. Panels (c) and (d) are for the three-dimensional Anderson model at different W with fixed $L = 1000$ and at different L with fixed $W = 1000$, respectively. The analytic result, i.e., Eq. (8), is also plotted for comparison. In the vicinity of $Dt = 2\pi, 4\pi$, we see that $|l(t)|$ approaches zero with increasing L or W.

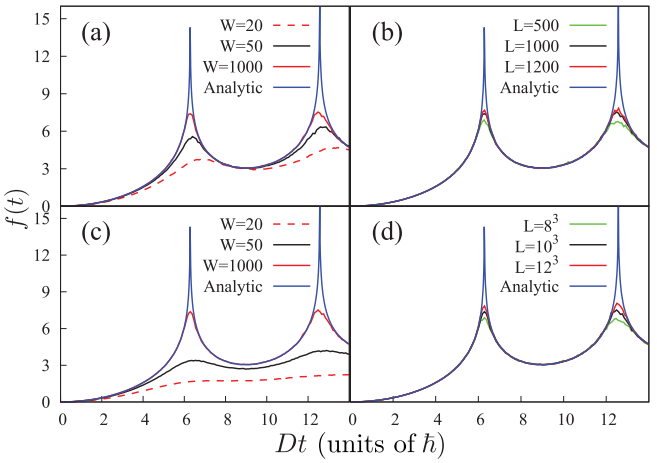

FIG. 2. Panels (a) and (b) plot the dynamical free energy $f(t)$ for the one-dimensional Anderson model at different W with fixed $L = 1000$ and at different L with fixed $W = 1000$, respectively. Panels (c) and (d) plot $f(t)$ for the three-dimensional Anderson model at different W with fixed $L = 1000$ and at different L with fixed $W = 1000$, respectively.

strength is strong ($W > 50$). For fixed W, the fit between numerics and Eq. (8) becomes even better as the system's size increases. As L increases, the minimum of $l(t)$ goes towards zero. We then expect that, in the limit $L \to \infty$, the Loschmidt echo does become zero at some critical times. And the value of the critical times also fits well with our prediction, i.e., $t_n^* D = 2\pi n$.

Figures 1(c) and 1(d) show the absolute value of the Loschmidt echo for the three-dimensional Anderson model at different W and L. In both one- and three-dimensional cases, the Loschmidt echo always fits Eq. (8) at large W, e.g., at $W = 1000$. By analyzing the change of $l(t)$ with increasing L, we also find in three dimensions that, in the limit $L \to \infty$, the single-particle Loschmidt echo becomes zero periodically at the critical times $t_n^* = 2\pi n/D$.

Next we discuss the dynamical free energy, whose nonanalyticity unambiguously defines the DQPTs and the critical times. The dynamical free energy is related to the single-particle Loschmidt echo by $f(t) = -\langle \ln(|l(t)|^2) \rangle$ where $\langle\rangle$ denotes the average over different disorder configurations.

Figure 2 shows the dynamical free energy at different L and W. Equation (9) is plotted at the same time for comparison, in which D is also averaged over different disorder configurations. The numerical results fit well with Eq. (9) at large W, e.g., at $W = 1000$ [see Figs. 2(a) and 2(c)]. As the disorder strength increases, the fit becomes even better. It is clear that the dynamical free energy displays a peak periodically at the critical times $t_n^* D = 2\pi n$. We also compare the dynamical free energy at different L. As the system's size increases, the peak of $f(t)$ becomes higher, and the shape of $f(t)$ is closer to that of Eq. (9) [see Figs. 2(b) and 2(d)].

The similar nonanalytic behavior of $f(t)$ has been observed in many other models, such as the XXZ model [19]. Here we would like to emphasize that the nonanalyticity of $f(t)$ in the Anderson models is caused by the localization-delocalization transition, different from the DQPTs caused by broken symmetries in the XXZ model [19] or by the close of the energy gap in the topological insulators [18].

At small W (e.g., at $W = 20$ for one dimension or at $W = 50$ for three dimensions), we see clearly the difference between numerics and Eq. (8) or (9) [see Figs. 1(a), 1(c) and 2(a), 2(c)]. This difference is caused by the failure of the two assumptions in the above derivation of Eqs. (8) and (9). First, the single-particle eigenstates are not δ like at small W so that their overlap with the initial wave function $[|\langle\phi(0)|\alpha_n\rangle|^2]$ deviates from $1/L$ but depends on $|\alpha_n\rangle$. Figures 3(a) and 3(b)

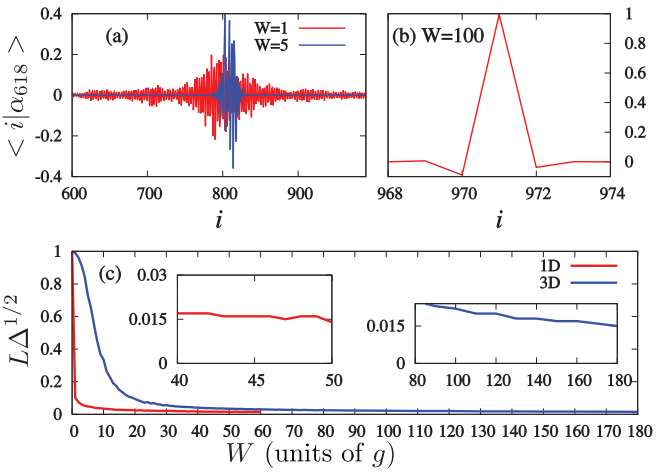

FIG. 3. Panels (a) and (b) plot the 618th eigen wave functions (count from the bottom of the spectrum) at different W with fixed $L = 1000$ for the one-dimensional Anderson model. i denotes the lattice sites. And the wave function is normalized as $\sum_{i=1}^{L} |\langle i|\alpha_{618}\rangle|^2 = 1$. Panel (c) plots $L\Delta^{1/2}$ as a function of W for the one- (red) and three-dimensional (blue) Anderson models.

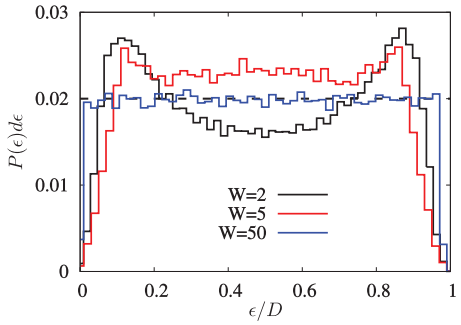

FIG. 4. $P(\epsilon)$ at different disorder strength. We select $d\epsilon = 0.02D$ and count the number of states in the interval $[\epsilon, \epsilon + d\epsilon]$. The dashed line represents the value of $P(\epsilon)d\epsilon$ as $P(\epsilon) = 1$ is a constant.

plot the eigen wave functions of the one-dimensional Anderson Hamiltonian at different W. At $W = 1$ and $W = 5$, the eigen wave function deviates obviously from the δ function, even if it is approximately the δ function at $W = 100$. We quantify the deviation of $|\langle\phi(0)|\alpha_n\rangle|^2$ from $1/L$ by defining the overlap variance

$$\Delta = \frac{1}{L^2}\sum_{n=1}^{L}\left(|\langle\phi(0)|\alpha_n\rangle|^2 - \frac{1}{L}\right)^2. \tag{10}$$

Δ is zero if $|\langle\phi(0)|\alpha_n\rangle|^2$ equals $1/L$ independent of $|\alpha_n\rangle$, but Δ is finite if $|\langle\phi(0)|\alpha_n\rangle|^2$ deviates from $1/L$. In Fig. 3(c), we see $\Delta = 1/L^2$ at $W = 0$ and decays towards zero as W increases. In one dimension, the overlap variance already decays to 0.015 at $W = 50$. But the decay of Δ is much slower in three dimensions, and it is at $W = 180$ when Δ decays to 0.015. This explains why the deviation of the numerics from the analytical results at small W is much larger in three dimensions than that in one dimension.

Second, $P(\epsilon_1,\epsilon_2,\ldots,\epsilon_L)$ in Eq. (7) is not a constant at small W. Since $P(\epsilon_1,\epsilon_2,\ldots,\epsilon_L)$ is a multivariate function which is difficult to plot, we alternatively plot $P(\epsilon) = \int d\epsilon_2\cdots d\epsilon_L P(\epsilon,\epsilon_2,\ldots,\epsilon_L)$ in Fig. 4, which is no more than the probability density of single-particle levels (or the normalized density of states). If $P(\epsilon_1,\epsilon_2,\ldots,\epsilon_L)$ is a constant, $P(\epsilon)$ must also be a constant. We see that $P(\epsilon)$ is approximately a constant as W is as large as 50, but apparently varies in the spectrum with two peaks at the edge and a valley at the center for small W (e.g., $W = 2$). This is not difficult to understand. At small W, the hopping term in the Hamiltonian (3) dominates. It is well known that the density of states has two peaks at the edge of the spectrum for the hopping Hamiltonian $\hat{H}_{\rm hop} = -g\sum_{\langle i,j\rangle}(\hat{a}_i^\dagger\hat{a}_j + \text{H.c.})$. But at large W, the random potentials in the Hamiltonian (3) dominate, leading to a constant density of states, as we argued below Eq. (7).

IV. WAVE FUNCTIONS BEFORE OR AFTER A ZERO OF THE LOSCHMIDT ECHO

We have shown that the Loschmidt echo has zeros $t_n^* = n2\pi/D$ at which the dynamical free energy becomes divergent. This indicates the DQPT according to definition. It was recently realized that a dynamical topological order parameter can be defined for some one- [17] or two-dimensional [26] topological systems. The dynamical order parameter has a jump at the critical time and then can be used to distinguish the quantum states before or after the DQPT. This motivates us to study the difference of the wave functions before or after the DQPT in the disordered systems.

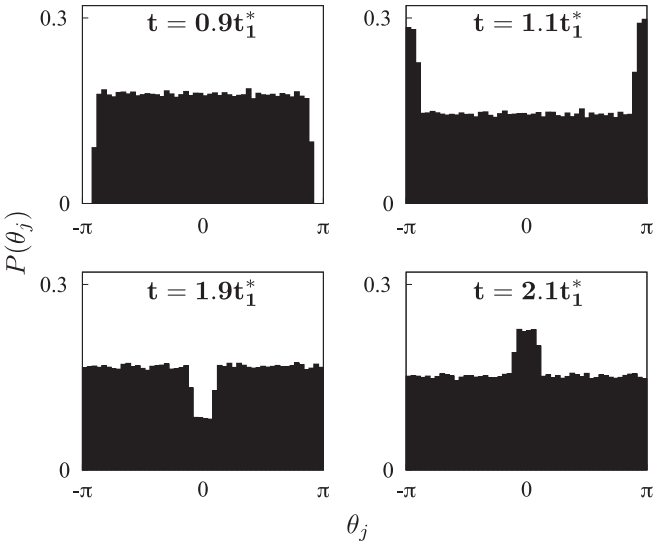

FIG. 5. Distribution of the principal phase of the wave function in the one-dimensional Anderson model. The four panels display $P(\theta_j)$ at different times with $t_1^* = 2\pi/D$ denoting the first critical time.

Let us consider the evolution of the single-particle wave function, starting from a plane wave of zero wave vector and quenched into the strongly disordered regime. The wave function can then be expressed by using Eq. (4). In the strong-disorder limit, the hopping term in the postquench Hamiltonian (3) can be neglected. It then becomes $\hat{H} = \sum_j u_j\hat{a}_j^\dagger\hat{a}_j$. The eigenstates of $\hat{H}$ are localized at each site j with the corresponding eigenenergies u_j. The time-dependent wave function becomes

$$|\phi(t)\rangle = \frac{1}{\sqrt{L}}\sum_j e^{-iu_jt}|j\rangle, \tag{11}$$

where we already used the fact $\langle j|\phi(0)\rangle = 1/\sqrt{L}$ for the initial wave function. At arbitrary time t, the magnitude of the wave function is a constant $1/\sqrt{L}$ everywhere. The phase of the wave function is $\theta_j = -u_jt$, which is a random number distributed uniformly in the range $[-Dt/2, Dt/2]$. If we consider the principal value of θ_j, which is limited in the range $(-\pi,\pi]$, its distribution $P(\theta_j)$ depends on time. In fact, the distribution of the principal phase can be used to distinguish the wave functions before or after a critical time.

In practice, we obtain $P(\theta_j)$ by first calculating the time-dependent wave function and then estimating the distribution of its phase over different sites. For each realization of the disorder potentials, we get one $P(\theta_j)$. The final distribution function is obtained by averaging over different disorder configurations for 100 times. We plot $P(\theta_j)$ at different t in Fig. 5, where we set $L = 1500$ and $W = 1000$. Note that $t_1^* = 2\pi/D$ is the first critical time and $t_2^* = 2t_1^*$ is the second one, etc. It is clear that the distribution function is a step function which is symmetric to $\theta_j = 0$. For $t < t_1^*$, $P(\theta_j)$ is

convex upward, or to be precise, the center of the curve (at $\theta_j = 0$) is higher than the edge (at $\theta_j = \pm\pi$). At $t = t_1^*$, the shape of $P(\theta_j)$ changes abruptly. It becomes convex downward for $t_1^* < t < t_2^*$; that is, the center is lower than the edge. But as t is beyond t_2^*, the distribution function becomes convex upward again. According to the shape of $P(\theta_j)$, the time-dependent wave functions can be classified into two types: convex upward and convex downward. Two types alternate at each DQPT.

V. CONCLUSION AND OUTLOOK

In this paper, we study the Loschmidt echo and the dynamical free energy after a quench of white-noise potentials. We find the periodically occurred dynamical quantum phase transitions with a period $2\pi/D$ where D is the width of the spectrum. By using the properties of the wave functions and the spectra in the strongly localized region, we argue that the dynamical free energy is divergent at DQPTs. We present numerical results in one- and three-dimensional Anderson models to support our arguments. Furthermore, we show that the distribution of the phase of the wave function can be used to distinguish the quantum states before or after each critical time.

Finally, we would like to mention that the measurement of the absolute value of the Loschmidt echo $|\mathcal{L}(t)|$ has been experimentally realized [20,21]. In a string of ions simulating interacting transverse-field Ising models by using Ca^+ ions, the nonequilibrium dynamics at DQPTs induced by a quantum quench is detected directly by measuring $|\mathcal{L}(t)|$ while projecting the many-body wave function at arbitrary time onto a chosen initial state [21]. With time-resolved state tomography, the topological DQPTs of ultracold atoms in optical lattices is measured by a full access to the evolution of the wave function [20]. In view of the experimental realization of the Anderson model in the optical lattice [27,28], we then expect that a new type of the nonanalyticity of the dynamical free energy caused by the localization-delocalization transition predicted in this paper can be observed in cold atoms.

ACKNOWLEDGMENTS

This work is supported by NSF of China under Grants No. 11304280, No. 11774315, and No. 11374266, and the Program for New Century Excellent Talents in University. S.C. is supported by the National Key Research and Development Program of China (2016YFA0300600) and NSFC under Grants No. 11425419, No. 11374354, and No. 11174360.

[1] P. W. Anderson, Phys. Rev. **109**, 1492 (1958).
[2] I. Bloch, J. Dalibard, and W. Zwerger, Rev. Mod. Phys. **80**, 885 (2008).
[3] M. Rigol, A. Muramatsu, and M. Olshanii, Phys. Rev. A **74**, 053616 (2006).
[4] M. Rigol, V. Dunjko, V. Yurovsky, and M. Olshanii, Phys. Rev. Lett. **98**, 050405 (2007).
[5] T. Caneva, E. Canovi, D. Rossini, G. E. Santoro, and A. Silva, J. Stat. Mech. **2011**, P07015 (2011).
[6] C. Gramsch and M. Rigol, Phys. Rev. A **86**, 053615 (2012).
[7] S. Ziraldo, A. Silva, and G. E. Santoro, Phys. Rev. Lett. **109**, 247205 (2012).
[8] S. Ziraldo and G. E. Santoro, Phys. Rev. B **87**, 064201 (2013).
[9] K. He, L. F. Santos, T. M. Wright, and M. Rigol, Phys. Rev. A **87**, 063637 (2013).
[10] M. Heyl, A. Polkovnikov, and S. Kehrein, Phys. Rev. Lett. **110**, 135704 (2013).
[11] C. Karrasch and D. Schuricht, Phys. Rev. B **87**, 195104 (2013).
[12] M. Fagotti, arXiv:1308.0277.
[13] E. Canovi, P. Werner, and M. Eckstein, Phys. Rev. Lett. **113**, 265702 (2014).
[14] F. Andraschko and J. Sirker, Phys. Rev. B **89**, 125120 (2014).
[15] J. M. Hickey, S. Genway, and J. P. Garrahan, Phys. Rev. B **89**, 054301 (2014).
[16] M. Schmitt and S. Kehrein, Phys. Rev. B **92**, 075114 (2015).
[17] J. C. Budich and M. Heyl, Phys. Rev. B **93**, 085416 (2016).
[18] S. Vajna and B. Dóra, Phys. Rev. B **91**, 155127 (2015).
[19] M. Heyl, Phys. Rev. Lett. **113**, 205701 (2014).
[20] N. Fläschner, D. Vogel, M. Tarnowski, B. S. Rem, D.-S. Lühmann, M. Heyl, J. C. Budich, L. Mathey, K. Sengstock, and C. Weitenberg, Nat. Phys. **14**, 265 (2018).
[21] P. Jurcevic, H. Shen, P. Hauke, C. Maier, T. Brydges, C. Hempel, B. P. Lanyon, M. Heyl, R. Blatt, and C. F. Roos, Phys. Rev. Lett. **119**, 080501 (2017).
[22] C. Yang, Y. Wang, P. Wang, X. Gao, and S. Chen, Phys. Rev. B **95**, 184201 (2017).
[23] B. L. Altshuler and B. I. Shklovskii, Zh. Eksp. Teor. Fiz. **91**, 220 (1986) [Sov. Phys. JETP **64**, 127 (1986)].
[24] F. M. Izrailev, Phys. Rep. **196**, 299 (1990).
[25] B. I. Shklovskii, B. Shapiro, B. R. Sears, P. Lambrianides, and H. B. Shore, Phys. Rev. B **47**, 11487 (1993).
[26] U. Bhattacharya and A. Dutta, Phys. Rev. B **96**, 014302 (2017).
[27] J. Billy, V. Josse, Z. Zuo, A. Bernard, B. Hambrecht, P. Lugan, D. Clément, L. Sanchez-Palencia, P. Bouyer, and A. Aspect, Nature (London) **453**, 891 (2008).
[28] G. Roati, C. D'Errico, L. Fallani, M. Fattori, C. Fort, M. Zaccanti, G. Modugno, M. Modugno, and M. Inguscio, Nature (London) **453**, 895 (2008).